Engineering and Applied Science Theses & Dissertations

McKelvey School of Engineering

Fall 12-20-2017

LS301 Fluorescence-guided Photodynamic Therapy of brain cancer using PpIX photosensitizer

Haini Zhang
Washington University in St. Louis

Follow this and additional works at: https://openscholarship.wustl.edu/eng_etds

⚙ Part of the Analytical, Diagnostic and Therapeutic Techniques and Equipment Commons, and the Biomedical Engineering and Bioengineering Commons

WASHINGTON UNIVERSITY IN ST. LOUIS

School of Engineering and Applied Science

Department of Biomedical Engineering

Thesis Examination Committee:
Samuel Achilefu, Chair
Monica Shokeen
Quing Zhu

LS301 Fluorescence-guided Photodynamic Therapy of brain cancer using PpIX photosensitizer

by

Haini Zhang

A thesis presented to the School of Engineering
of Washington University in St. Louis in partial fulfillment of the
requirements for the degree of
Master of Science

December 2017

Saint Louis, Missouri

Contents

Acknowledgments

Haini Zhang

Washington University in St. Louis
December 2017

Dedicated to my parents.

I cannot be more thankful to my parents for supporting me for everything. To my father, I would like to express my thanks for being a good friend and helping me go through all the difficulties. To my mother, I appreciate it lot for helping me through my grow up. I would also like to thank to my brother, for cheering me up at any situations.

ABSTRACT OF THE THESIS

A Mock Thesis on the Proper Formatting of Theses and Dissertations

for Engineering-based Grad Students

by

Haini Zhnag

Master of Science in Biomedical Engineering

Washington University in St. Louis, 2017

Research Advisor: Professor Samuel Achilefu

Incomplete brain tumor removal always causes neurologic deficit, disease recurrence and high mortality. Protoporphyrin IX (PpIX) accumulated in glioma cells with exogenous 5-aminolevulinic acid (5-ALA) serves as contrast agent for fluorescence-guided surgery and as well as acts as a photosensitizer for photodynamic therapy (PDT). However, the accurate tumor delineation using PpIX is limited by autofluorescence and superficial penetration depth. LS301 is a tumor-targeted near-infrared (NIR) contrast agent developed in our lab which allows deeper tumor imaging and avoids autofluorescence. My project aims to investigate whether LS301 can improve PpIX mediated PDT and tumor removal surgery. We have demonstrated co-localization of LS301 and PpIX in DBT and U87-MG glioma cell lines and are currently testing the effect of LS301 on PpIX mediated PDT in vitro. We will also compare LS301-PpIX with PpIX only PDT and tumor removal in mouse models of brain cancer. This study can potentially increase efficacy of PDT and fluorescence-guided brain tumor resection.

Chapter 1

Introduction

1.1   Brain cancer and conventional brain tumor removal surgery

Brian cancer is one of the top ten leading cause of cancer death in the United States [1]. From the 2017 cancer statistics, brain and other nervous system cancer account for 3% of all cases in men and women, respectively [1]. Moreover, relative five-year survival for brain cancer has hardly improved for thirty years and the survival rate for all malignant brain tumor patients is only 30% [1]. Particularly, the survival rate for the most common form of primary malignant brain tumors, glioblastoma, is only 5.5% [1]. In addition, brain cancer also represents 20% of all cancer cases in child [2]. In most recent surveys, brain cancer is the leading cause cancer death in children (0-14 years old age) [3]. There are many methods to treat brain tumor and brain tumor removal surgery is one modality. The application of image guidance system is prevailing in brain tumor removal surgery. Conventionally, brain tumor surgery with image guidance system still uses surgery microscope shown in Fig 1.1 [4]. Surgery microscope is a high-cost and huge installation in the operation room. And the surgery microscope is difficult to be rotated and twisted with the movement of surgeon's head, thereby some tumors cannot be found and removed during the surgery, especially those diffuse tumor and boundary tumor cells surrounded by healthy tissue [4]. Instead, incomplete tumor removal during surgery can cause local cancer recurrence, paralysis, low intelligence quotient and high mortality in brain tumor patients. Thus, improving the extent of tumor resection may increase long term survival and decrease the need for radiation and chemotherapy along with its harmful side-effects. One strategy to improve tumor resection is to use real-time fluorescence image guidance.

Figure 1.1 surgery microscope in operation room

1.2   Binocular goggle augmented imaging system

To identify microscopic tumors, Dr. Samuel Achilefu and Optical Radiology lab has developed a wearable binocular goggle augmented imaging and navigation system (GAINS) [5]. GAINS provides more accurate intraoperative visualization of tumors to improve surgical outcomes and reduce the rate of surgery repeats. With the application of real-time fluorescent image system, GAINS can quickly produce images and allow surgeons to visualize and distinguish the marginal and diffuse tumors from healthy tissues [5]. Besides, GAINS can mitigate the difficulties and inconvenience of surgery microscope in brain tumor removal surgery. The wearable goggle imaging system is demonstrated in Fig 1.2 [5].

Figure 1. 2 Wearable goggle imaging system

1.3　5-Aminoleulinic acid (5-ALA) and LS301 in clinical use

A contrast agent is necessary for fluorescence image guided surgery. Protoporphyrin IX (PpIX) is the metabolism product of 5-Aminoleulinc acid (5-ALA) in heme biosynthesis pathway serving as a fluorophore compound when excited by appropriate excitation light[6]. The heme biosynthesis pathway is illustrated in fig 1.3 [6].
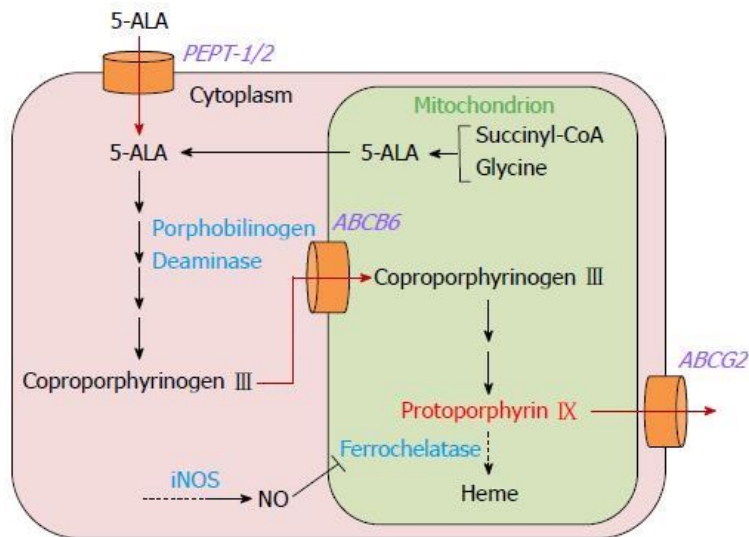

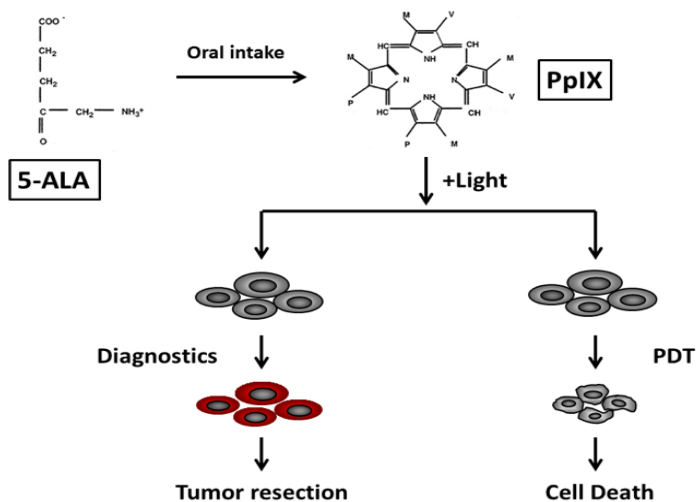**Figure 1.3 Metabolic pathway of 5-ALA**

Figure 1.4 Schematic representation of clinical use of 5-ALA

PpIX is particularly accumulated in heme biosynthesis pathway because the inactivity of ferrochelatase , in tumor cells. Ferrochelatase is the crucial enzyme at the final step of the heme biosynthesis [6]. 5-aminoleulinc acid (5-ALA) has been approved in Europe for high grade brain tumor, such as glioblastoma. PpIX fluorescence has been not only used for intraoperative contrast under blue light for malignant glioma but also be used as a photosensitizer for photodynamic therapy (PDT) to cause cytotoxic cell death [7]. The overall flowchart of 5-ALA in clinical use is shown in fig. 1.4 [7].

However, there are many limitation of 5-ALA in clinical use. The optimal excitation wavelength of PpIX is 405nm, but it has low permeability for visualizing superficial tumor cells at this short wavelength light. Even though 635nm wavelength excitation light can penetrate deeper into the tissue, PpIX has very weak absorption at this wavelength light. PpIX fluorescence is affected by autofluorescence as well. These limitations of 5-ALA induced PpIX often lead to inappropriate power delivery for PDT leasing to inadequate cytoxicity in tumor tissue or substantial toxicity in healthy tissue. Superficial PpIX may also lead to incomplete tumor removal due to inaccurate estimation of tumor extent. Dr Achilefu has developed a near-infrared fluorescence probe LS301 that has been shown to be highly cancer targeted [9]. LS301 can target different types of covering

breast cancer, lung cancer, pancreatic cancer etc [8]. The absorption and emissions spectrum o LS301 and PpIX are shown in fig 1.5 [7,8,9]. This project aims to investigate whether LS301 fluorescence can improve PpIX PDT and increase surgical removal of brain tumors.
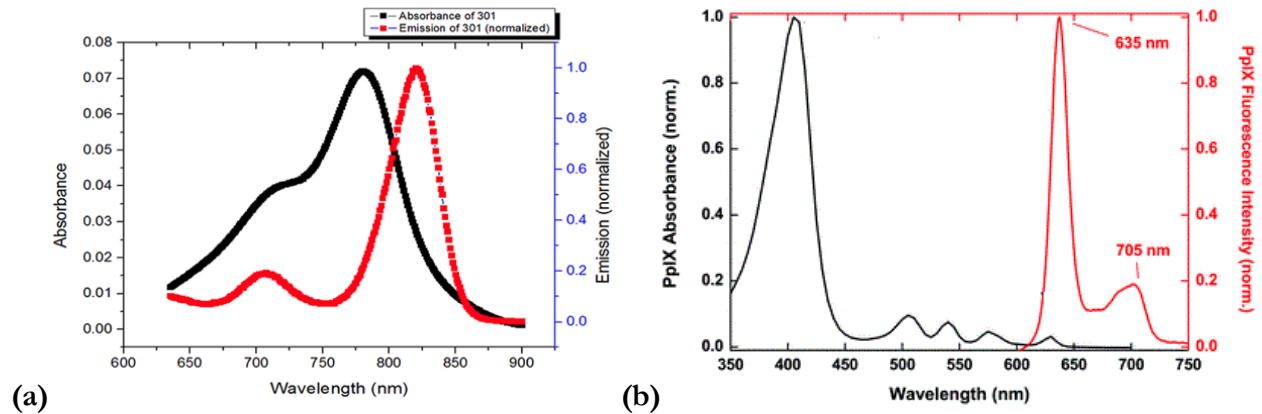
Figure 1.5 Absorption and Emission spectrum of LS301 and PpIX, (a) LS301 spectrum and (b) PpIX fluorescence spectrum.

1.4   Fluorescence lifetime imaging

To minimize the interference of autofluoresence in PpIX fluorescence detection, we introduced fluorescence-lifetime imaging (FLIM) in this project. FLIM is relaying on the differences in the exponential decay rate of the fluorescence emission [10]. The mechanism of FLIM is shown in fig 1.6 [10]. Fluorescence lifetime is independent to the concentration of compounds.

(a)   **(b)**

Figure 1.6 Fluorescence lifetime mechanisms

The fluorescence lifetime of 5-ALA induced PpIX has been identified to be around 6 ns and other intermediate metabolites generate a significantly different fluorescent lifetime at around 1ns, which shown in fig.1.7 [11]. Therefore, 5-ALA induced PpIX fluorescence is distinguishable from autofluoresence by FLIM.

Figure 1.7 PpIX and autofluorescence lifetime

Chapter 2

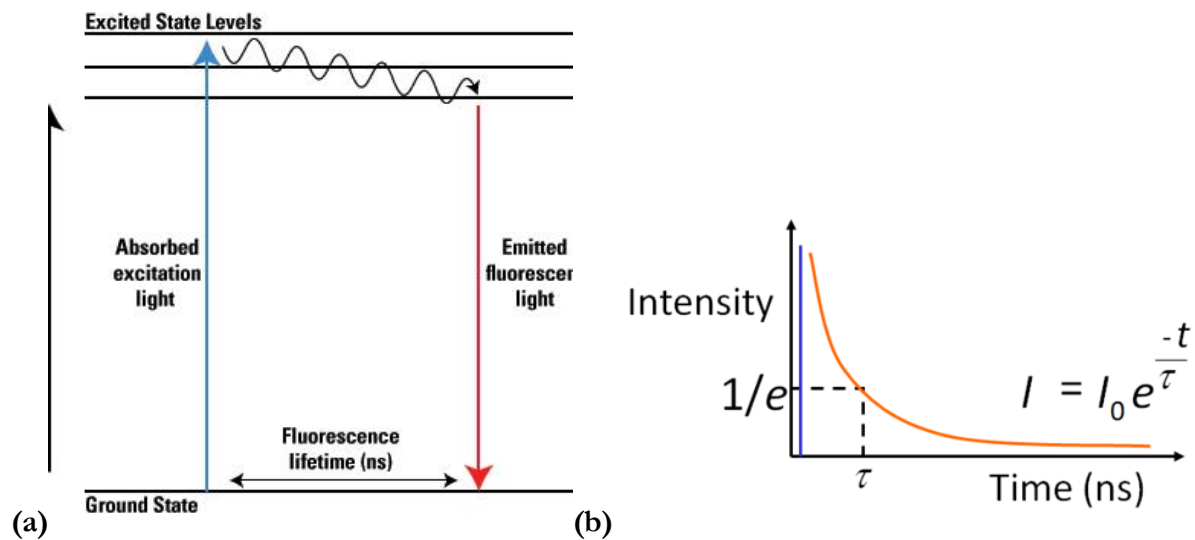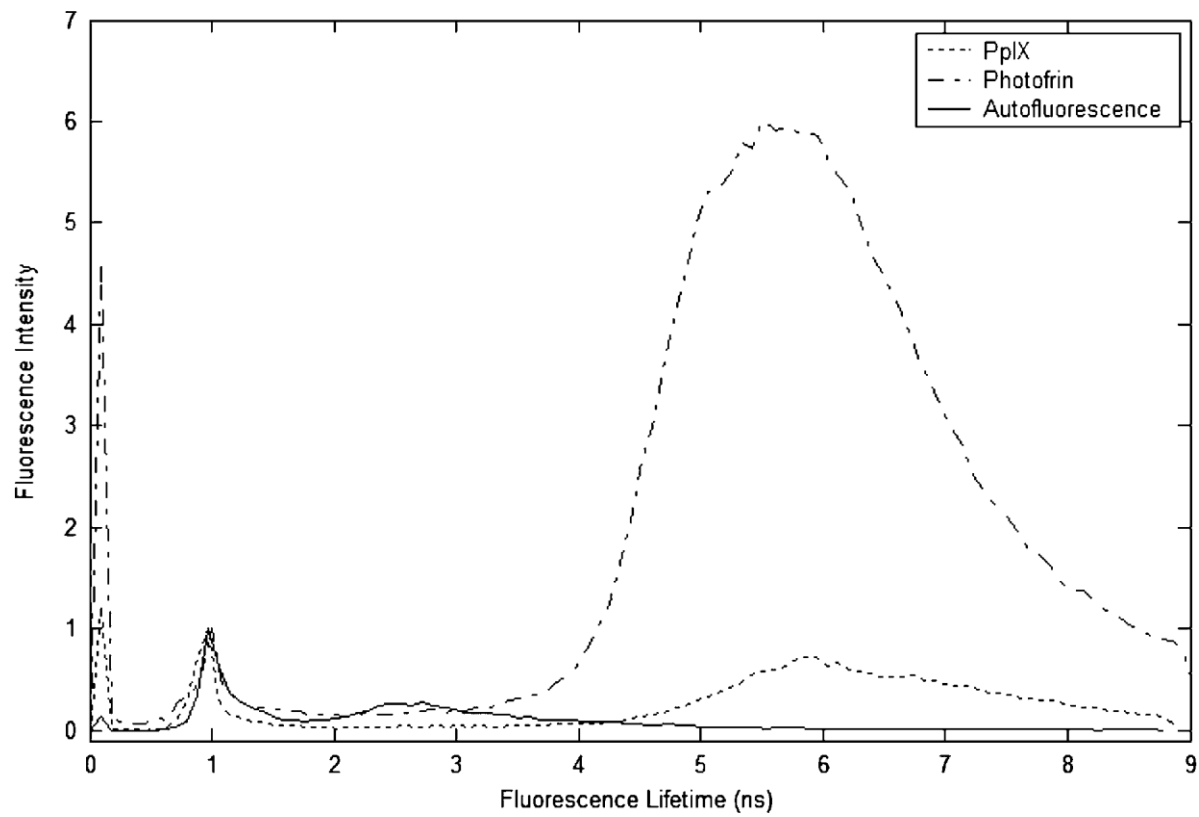# Materials and Methods

2.1 Cell lines

U87-MG human brain glioblastoma cells (ATCC, HTB-14, Mamassas, VA, USA) were cultured in Eagle's minimum essential medium (RMPI 1640) with L-glutamine (Lonza, Poetmouth, NHUSA), 1% penn-strep and 10% fetal bovine serum (PAA, Westborough, MA, USA) at 37°C and 5% CO_2. DBT glioblastoma were cultured in DMEM with L-glutamine (Lonza, Poetmouth, NH, USA), 1% penn-strep and 10% fetal bovine serum (PAA, Westborough, MA, USA) at 37°C and 5% CO_2.

2.2 *In vitro* fluorescence measurement

2.2.1 Confocal microscope

Seeded 30,000 cells in 8 chamber culture slides in medium overnight. Treated cells with 4mM 5-ALA only, 4uM LS301 only and both 4mM 5-ALA and 4uM LS301 for 6 hours, respectively. PpIX and LS301 fluorescence were measured using Olympus confocal microscope fv1000, 60X magnification at 488/ 630 nm and 780/800 nm, respectively. Fluorescence intensity was calculated by ImageJ.

2.2.2 Microplate reader

5-ALA (Sigma-Aldrich, St. Louis, MO, USA) was dissolved in phosphate buffered saline (ref.) to make a 50.0mM solution. 100 uL of cells were plated in each well in black wall and clear bottomed 96 well plates with a density of 10,000 cells per well. Cells were treated with 5-ALA solution at 50.0, 25.0 12.5, 6.25, 3.13, 1.56, 0.78, 0.39, 0.20, 0.05, 0.02 mM for 3 hours. Cells per well were treated

with 4mM 5-ALA and 1uM LS301 (Achileful Optical radiology lab, Wustl, MO, USA) for 0, 8h, 16, 24, 32, 48, 56, 64, 72 hours, respectively. 96 wells plates with treated cells were measure using a Microplate Reader, with a standard 405nm excitation/ 635nm emission filter to detect PpIX fluorescence and 780nm excitation/ 830nm emission filter to detect LS301 fluorescence, respectively.

2.2.3 Fluorescence analysis on FLIM

30,000 cells were seeded in the dish culture and cells were treated with 8mM 5-ALA for 24 hours. 4uM LS301 was further used to treat the cells for another 6 hours. Control wells, as well as 5-ALA and LS301 treated only were also prepared. PpIX fluorescence was recorded by 519LP excitation and LS301 fluorescence was recorded by 790/LP filter. The resolution was set to 400 X 400 pixels. Fluorescence analysis was then merged by ImageJ.

2.3 Subcutaneous and orthotopic mice models

2.3.1 Small animal imaging

Around 1.5 million DBT and U87 tumors cells were implanted subcutaneously into the right flank of BalbC and Nude mice models, respectively. Orthotopic 87-MG mice were offered by LeMoyne Habimana-Griffin at ORL center, WUSTL. After the tumor grew big enough, 100 uL of 60uM LS301 was injected intravenously. After 16 hours, 100uL of 50mg/mL 5-ALA dissolved in PBS was injected intraperoneally (IP). FMT, Brucker carestream multiple spectral fluorescence imaging and Pearl Trilogy small imaging system were used to obtain fluorescence images. Mice were imaged by channel 700 (excitation 685nm, emission 720nm) and channel 800 (excitation 785nm, emission 820 nm) on Pear imager at dorsal position and ventral position, respectively. PpIX fluorescence were also imaged by Brucker imaging system using 420nm excitation/ 600nm emission, 510nm excitation/600nm emission, 630nm excitation/700nm emission, respectively. And LS301 fluorescence detection on Brucker used 780nm excitation/830nm emission. PpIX and LS301

fluorescence calibration was set on FMT by 635 nm excitation/ 650-670nm emission and 790nm excitation/ 805+ nm emissions, respectively.

2.3.2   Photodynamic therapy protocol

Five nude mice were used for PDT experiment. All five mice were implanted with U87 cells. After the tumor grown for three weeks, injected 100uL 60uM LS301 in M4 and M5 and then injected 100uL, 50mg/mL 5-ALA after 16h hours. M2 and M3 were only injected with 100uL 50mg/mL 5-ALA. M1 was used as control without any treatment. 660nm laser was used to irradiate the tumor spot after 6 hours post injection of 5-ALA in M2, M3, M4 and M5. The distance between LED lends and mice tumor was set to 10 cm to generate an intensity of $72mW/cm^2$ irradiation. Exposure time was 20 minutes [12]. The size of tumors was measured and recorded for 5 days.

2.3.3   ImageJ analysis

All the analysis of fluorescence intensity *in vivo* and *in vitro* experiments were analyzed by ImageJ. Data were plotted by using Prim's algorithm.

Chapter 3

Results and Discussion

3.1 *In vitro* study

### 3.1.1 LS301 has good uptake in DBT and U87 cells

Initially, we identified the uptake of LS301 and 5-ALA in two cell models, U87 and DBT cells. U87 is high grade IV human adult glioblastoma cell line and DBT is high grade IV mouse glioblastoma cell line, respectively. PpIX fluorescence failed to be observed on the Confocal in our lab due to the absence of ideal 405nm/635nm excitation/emission filter. In addition, no significant difference of PpIX fluorescence between 5-ALA treated U87 and DBT cells and control cells under 488nm/635nm, 580nm/640nm and 615 nm/715 nm filters on confocal (Fig. 3.1 a-f). PpIX fluorescence was even weak at the ideal 405nm/635nm excitation filter on confocal which offered by the Molecular Imaging Center at Washington University (Fig 3.1 g). LS301 fluorescence in DBT and U87-MG cells treated with 4uM LS301 for 6 hours were distinct on Confocal microscope by using 780nm excitation and 830 emission filters (Fig. 3.2). Thus, we made a conclusion that LS301 has a better uptake in the two cell lines than 5-ALA.

(a)

(b)

(c)

(d)

(e)

(f)
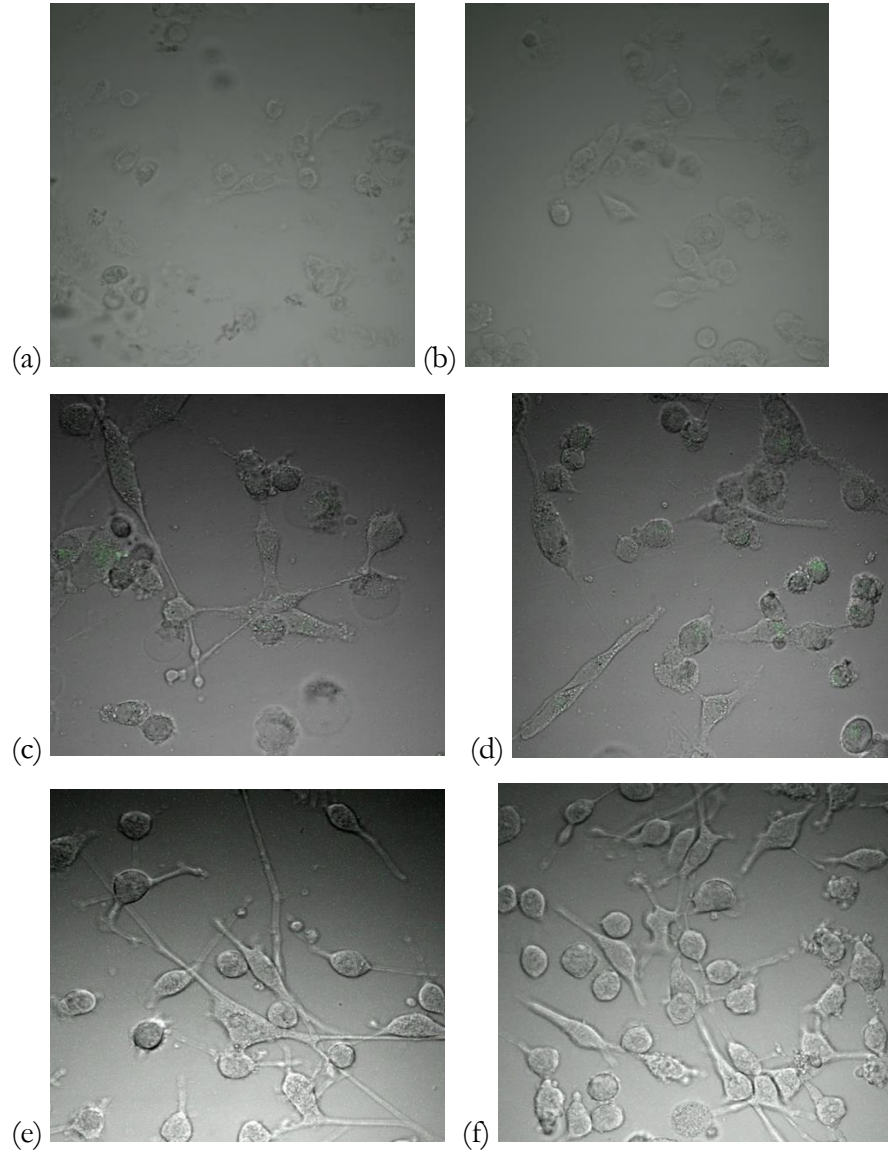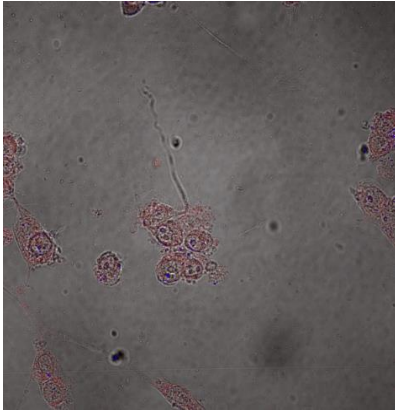
(g)

Figure 3.1 PpIX fluoresence in U87 cell line by Confocal microscope .(a, c, e) Fluoresence signal in control 87-MG cells at 488nm exictation/ 635nm emission filter, 580 nm exictation/ 640nm emission filter 615nm exictation/ 715 nm emission filter, repectively. (b,d,f), PpIX fuorescnece in U87-MG cells treated with 0.4 mM 5-ALA for 6 hours at 488nm excitation/ 635nm emission filter filter, 580 nm exictation/ 640nm emission filter 615nm exictation/ 715 nm emission filter, repectively. (g) PpIX fuorescnece in U87-MG cells treated with 0.4 mM 5-ALA for 3 hours at 405 nm excitation/ 635nm emission filter.
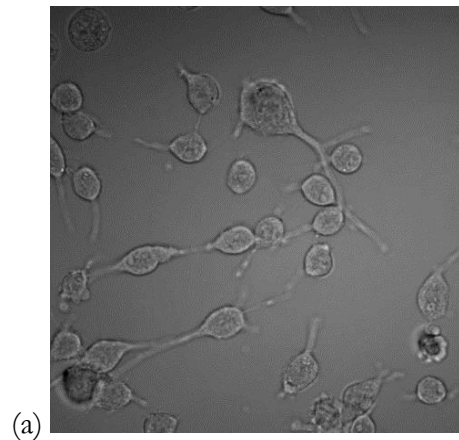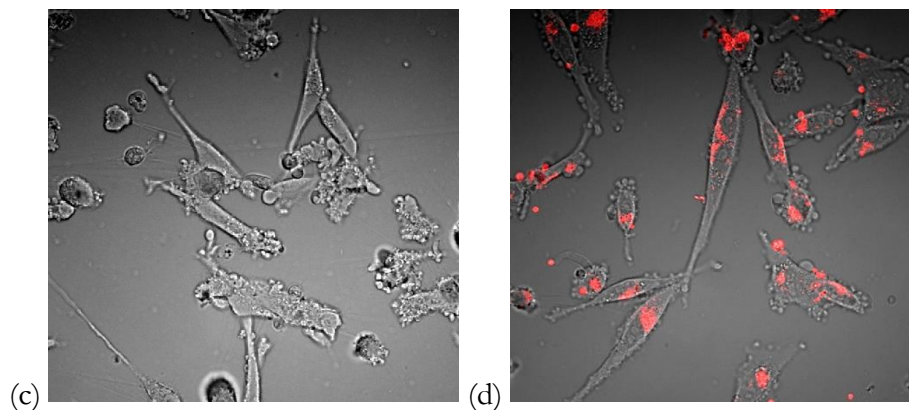

(a)
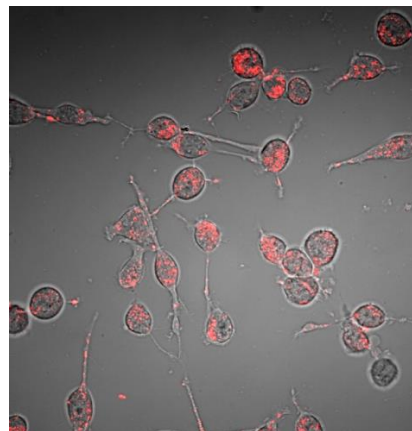
(b)

Figure 3.2 LS301 fluoresence in U87 and DBT cell lines by Confocal microscope. (a) Fluorescnece in untreated DBT cells (control) and (b) LS301 fluoresence (red) in DBT cells treated with 4uM LS301 for 6 hours by 785 nm/830nm filter. (c) Fluorescnece in untreated U87 cells (control) and (d) LS301 fluoresence (red) in U87 cells treated with 4uM LS301 for 6 hours by 785 nm/830nm filter.

3.1.2 LS301 and PpIX fluorescence quantification by microplate reader

We further studied the uptake of LS301 and 5-ALA in DBT and U87 cell lines by using microplate reader. The microplate reader provides the best choice of excitation and emission filter, 405nm/635nm, for PpIX fluorescence. The results showed that the optimum concentrationof 5-ALA for both DBT and U87-MG was 4mM. Also, DBT cells had a better uptake of 5-ALA than U87 cells. (Fig. 3.3). At the concentration of 5-ALA at 4mM, PpIX fluorescence was over 30 times higher in DBT cells than untreated cells but only two fold higher in U87 cells over untreated cells. The optimum LS301 concentration was 4uM. LS301 was produced in Dr. Achilefu's lab and it was sparing used in the experiment. The highest concentration of LS301 for quantifying the LS301 fluorescence was 5uM. For both DBT and U87 cell lines, LS301 fluorescence intensity in 0.4uM LS301 treated cells was already 10 folds higher than untreated cells. From the fig. 3.3 and fig. 3.4, both DBT and U87 cells demonstrated better uptakes of LS301 than 5-ALA. The uptake of LS301

and 5-ALA over time was also studied. The error bar in the fig 3.5 is scientifically large. The time course experiment will be repeated in the future.
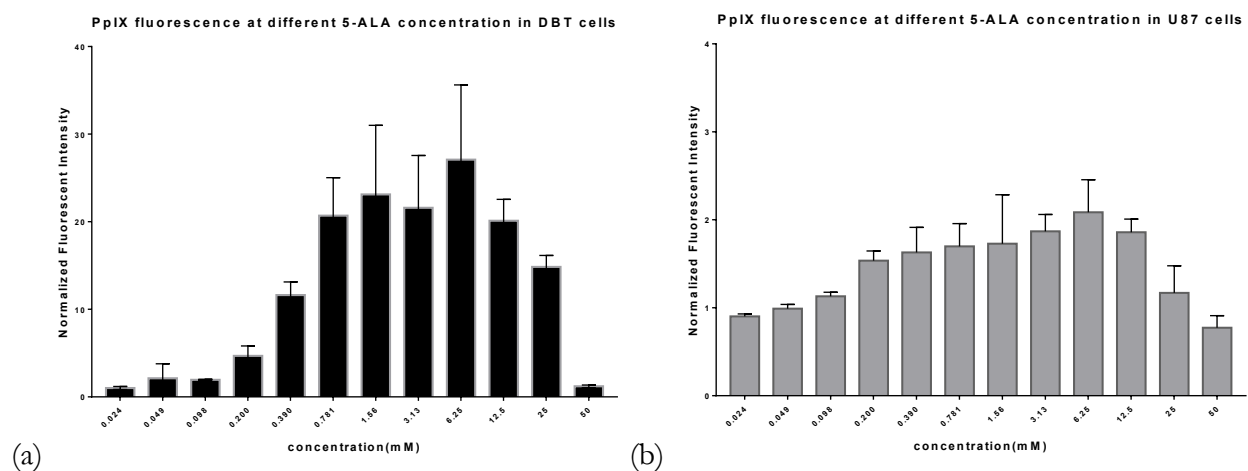

(a)   (b)

Figure 3.3 Optimum concentration of 5-ALA for inducing PpIX is 4mM. (a), (b) PpIX fluorescence intensity at increasing 5-ALA concentrations in DBT and U87 cell lines for 3 hours, respectively. Excitation at 405nm and emission at 635nm on microplate reader were used for PpIX fluorescence.
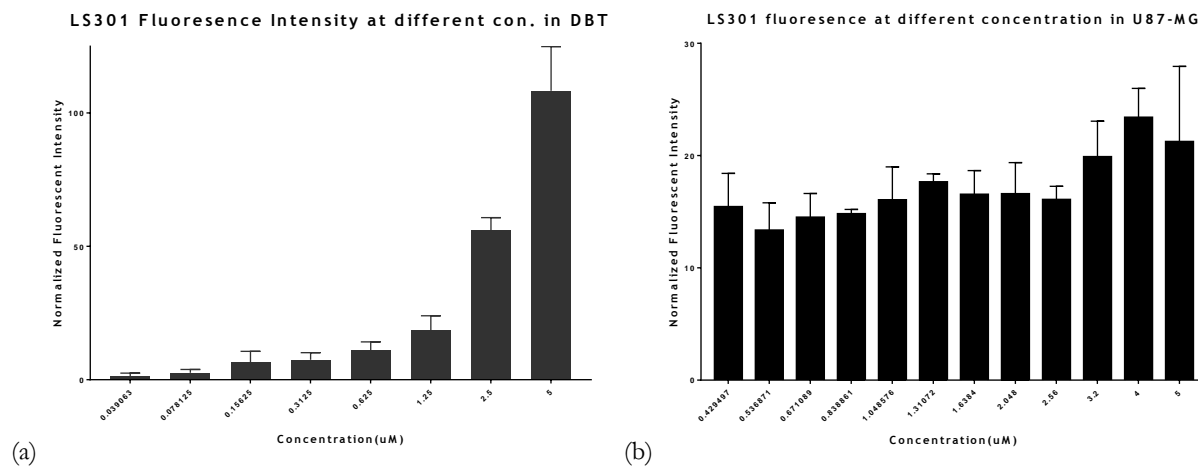

(a)   (b)

Figure 3.4 Optimum concentration of LS301 is 4uM. (a), (b) LS301 fluorescence intensity at increasing LS301 concentration in DBT and U87 cell lines for 3 hours, respectively. Excitation at 780 nm and emission at 830 nm on microplate reader were used for PpIX fluorescence.
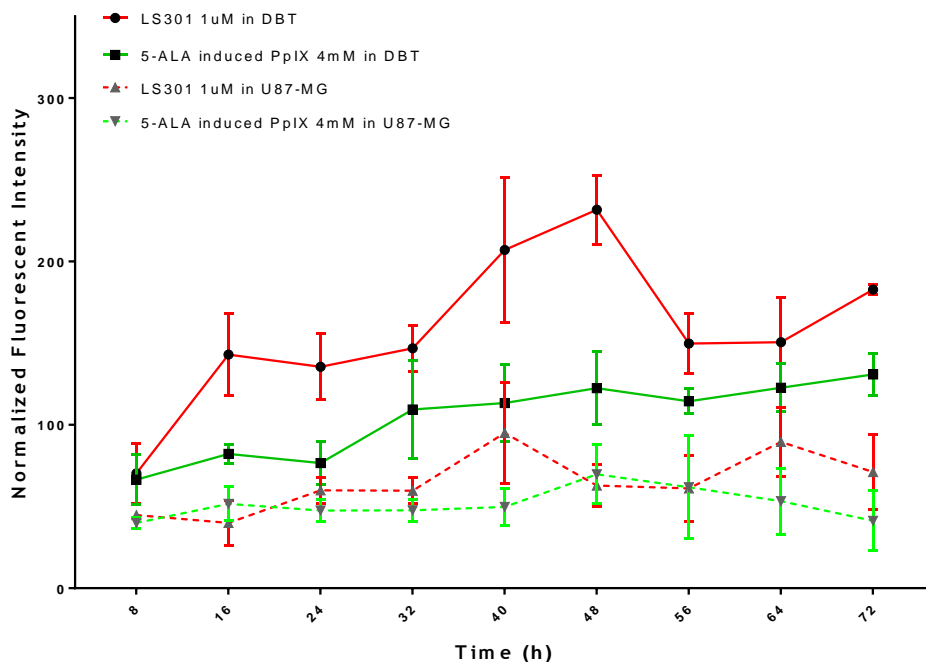
Fig 3.5 LS301 and 5-ALA uptake time course recorded on microscope reader. LS301 fluorescence intensity change at 780nm/830nm filter 72 hours in DBT cells (solid red line) and U87 cells (dash red line) after treated with 1uM LS301, respectively. PpIX fluorescence intensity at 405nm/635nm filter change over 72 hours in DBT cells (solid green line) and in U87 cells (dash green line) after treated with 4mM 5-ALA, respectively.

3.2   Fluorescence lifetime imaging analysis

Autofluoresence in DBT and U87 at 510nm excitation filter gave the average fluorescence life time at around 2ns. Average fluorescence life time for both cell lines treated with 8mM 5-ALA was around 4ns (Fig 3.5 and Fig 3.7). The fluorescence lifetime of PpIX is slightly different from the study of Jennifer A. Ressell et al because the autofluorescence is not removed in the FLIM measurement. The LS301 average fluorescence life time was around 1ns. (Fig 3.5 and Fig.3, 7) Image J analysis showed the co-localization of LS301 and PpIX. (Fig 3.6 and Fig 3.8). To further confirm the co-localization of LS301 and PpIX in cells, the bio-distribution of LS301 and PpIX in different

organelles will be studied in the future. Overall, LS301 and PpIX show co-localization at some sites inside of U87 and BDT cells.
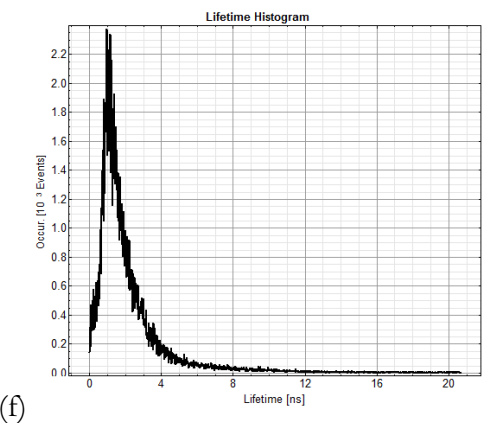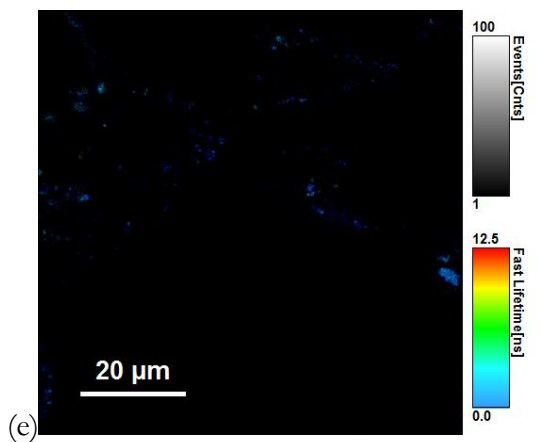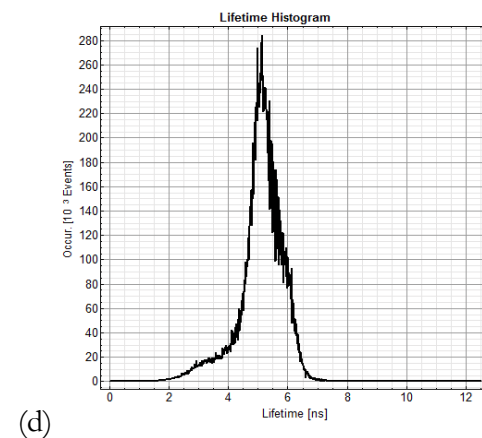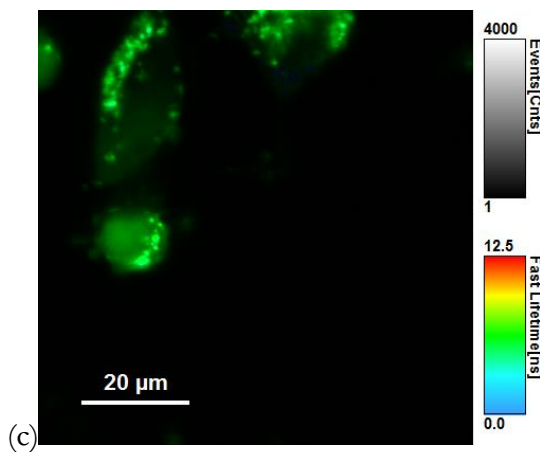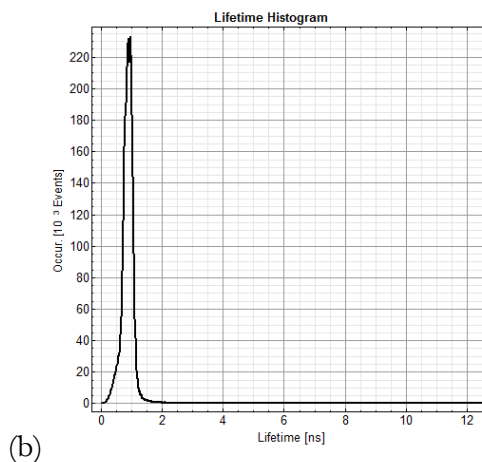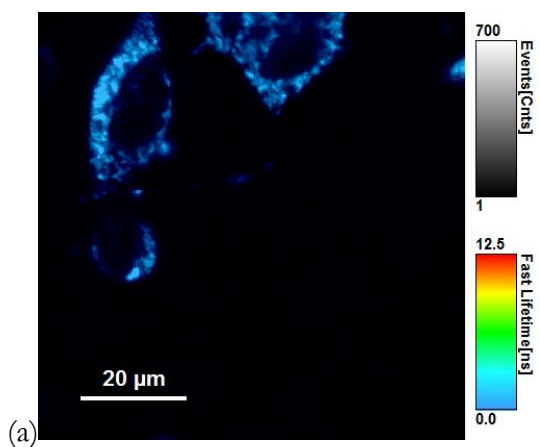
Figure 3.5 Fluorescence lifetime for LS301 and PpIX in DBT cells. (a) and (b): Fluorescence lifetime image and lifetime histogram of LS301 in DBT cells, receptively. (c) and (d): Fluorescence lifetime image and lifetime histogram of PpIX in DBT cells at 510nm excitation light filter, receptively. (e) and (f) Fluorescence lifetime image and lifetime histogram of autofluorescence in DBT cells at 510nm excitation light filter, receptively.
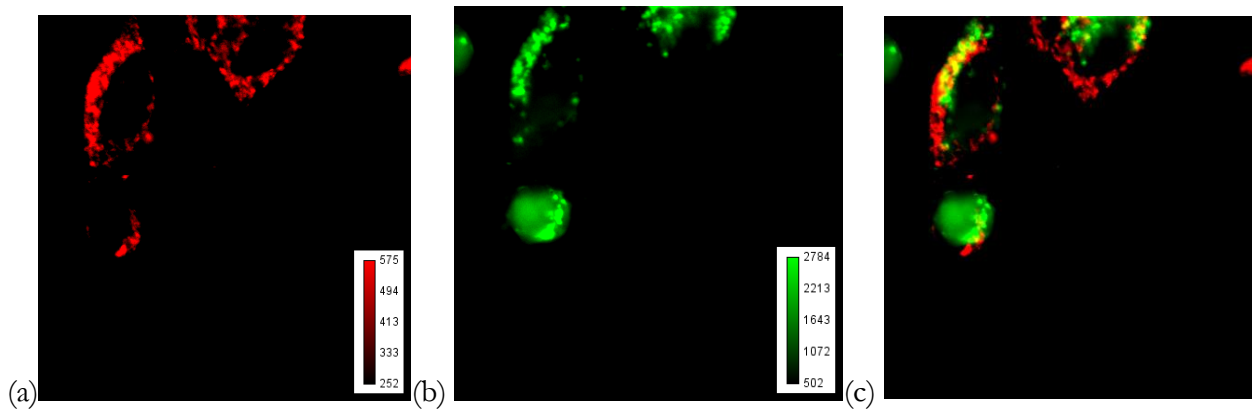

Figure 3.6 LS301 and PpIX fluoresence in same DBT cells. (a) LS301 fluoresence in DBT cells (b) PpIX fuoresence in DBT cells. (c) overlap of LS301 and PpIX fluoresence in DBT cells on imageJ.
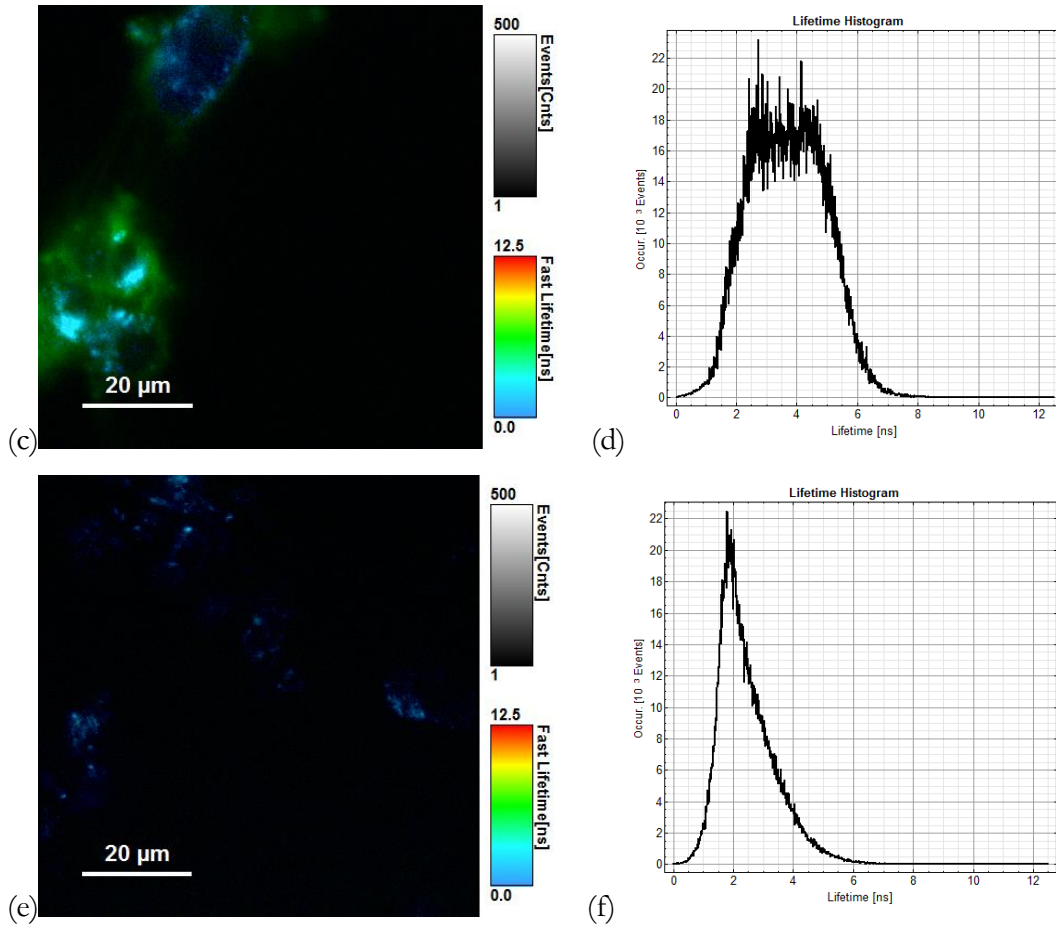
Figure 3.7 Fluorescence lifetime for LS301 and PpIX in U87 cells. (a) and (b): Fluorescence lifetime image and lifetime histogram of LS301 in U87 cells, receptively. (c) and (d): Fluorescence lifetime image and lifetime histogram of PpIX in U87 cells at 510nm excitation light filter, receptively. (e) and (f) Fluorescence lifetime image and lifetime histogram of autofluorescence in U87 cells at 510nm excitation light filter, receptively
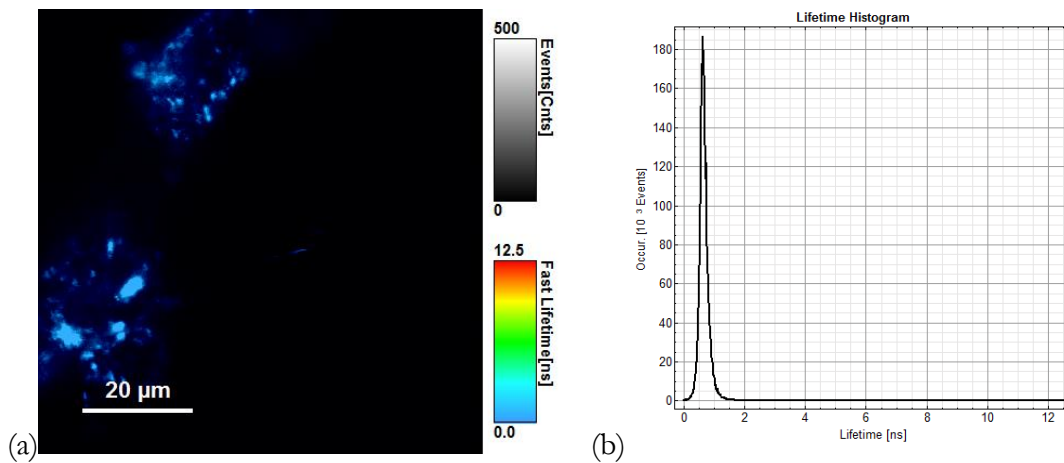
Figure 3.8 LS301 and PpIX fluoresence in same U87 cells. (a) LS301 fluoresence in U87 cells (b) PpIX fuoresence in U87 cells. (c) overlap of LS301 and PpIX fluoresence in U87 cells on imageJ.

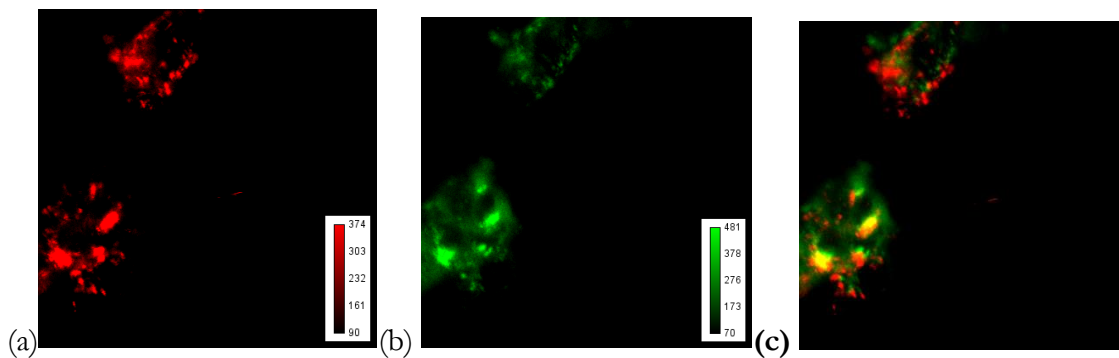# 3.3 LS301 and PpIX co-localization in mice model

3.3.1 Subcutaneous DBT mice

Identification of LS301 and PpIX fluorescence was then confirmed in mice modes with DBT tumors implanted subcutaneously. Three different excitation/emission filtered lights were used on Bruker multi-spectra fluorescence imaging system, 420nm/600nm, 510nm/600nm and 630nm/700nm, respectively. 5-ALA induced PpIX fluorescence was only detectable by 630nm excitation filtered light (Fig 3.9). This phenomenon can be explained by the permeability of light though tissue: longer wavelength light is capable for deeper detection. Merging the PpIX fluorescence at 630nm excitation filter and the LS301 fluorescence at 760nm excitation light by using ImageJ analysis which showed the overlap of LS301 and PpIX fluorescence in subcutaneous DBT mouse at tumor area. (Fig 3.10). PpIX fluorescence was recorded at different time after the injection of 5-ALA, which is shown in fig. 3.11. There is not significantly change over time by 420nm/600nm and 510nm/600nm filters. However, PpIX fluorescence was increased with increased time after 5-ALA inject and reached at maximum after the skin was deflected at the DBT tumor area (Fig. 3.11). In addition, PpIX fluorescence of biodistribution by the three different filters also indicates that 630nm/700nm filter is the optimal choice for visualizing PpIX fluorescence *in vivo* (Fig 3.14). Figure 3.12 shows the overlap of LS301 and PpIX fluorescence at the tumor area after skin deflected. Biodistribution of PpIX and LS301 in organs show that LS301 and 5-ALA induced PpIX mainly accumulate in the DBT tumor tissue and so as to overlap of LS301 and PpIX in the tumor tissue (Fig. 3.13). Besides, high fluorescence in tumor and low fluorescence in muscle means high contrast. The tissue-to-muscle ratio of LS301 in Table 3.1 is two folds higher than PpIX (630nm/700nm). This proves that LS301 has higher contrast which could be potentially used to guide PpIX imaging surgery.
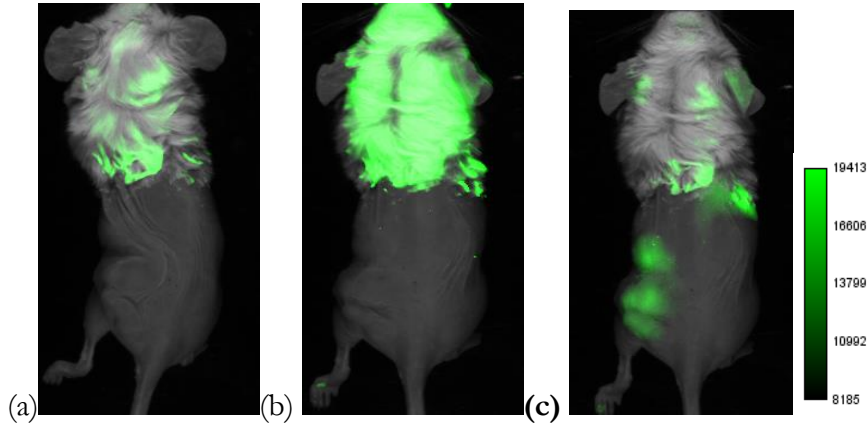
Figure 3.9 PpIX fluoresence was not detectable at 420nm/600nm filtered light (a), 510nm/600nm filtered light (b) and 630nm/700nm filtered light (c), respectively.
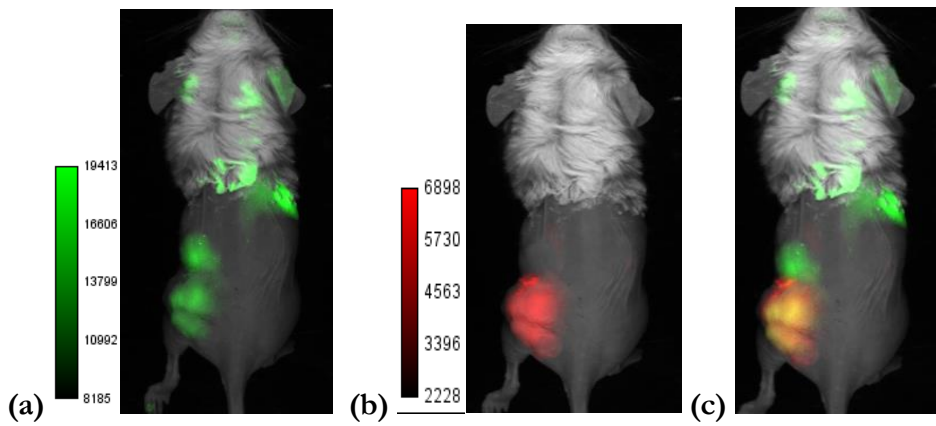

Figure 3.10 LS301 and PpIX fluoresence overlap in subcutaneous DBT mouse. (a) PpIX fluoresence (green) by 630nm/700nm filtered light (b) LS301 fluoresence (red) by 760nm/700nm filtered light. (c) Merged LS301 and PpIX fluorescence by Image J.

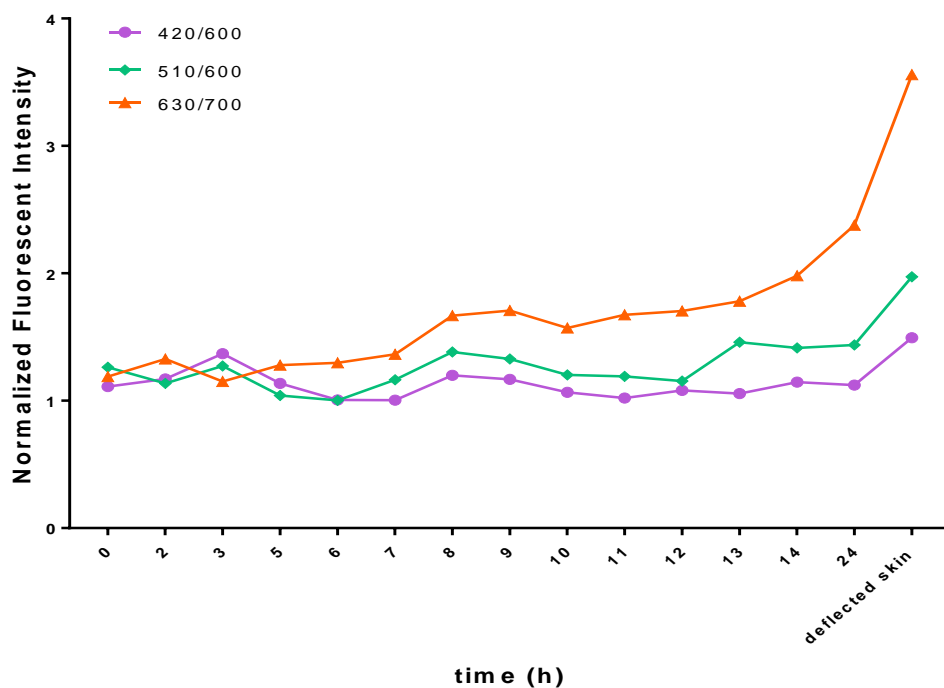# 5-ALA induced PpIX fluorescence at three different ex/em

Figure 3.11: 5-ALA induced PpIX fluorescence intensity at different time by three different excitation/emission filters, 420nm/ 600nm (purple), 510/600nm (green) and 630nm/700nm (orange), repectively. PpIX fluoresence intensity after the skin deflected over the tumor area was also shown.
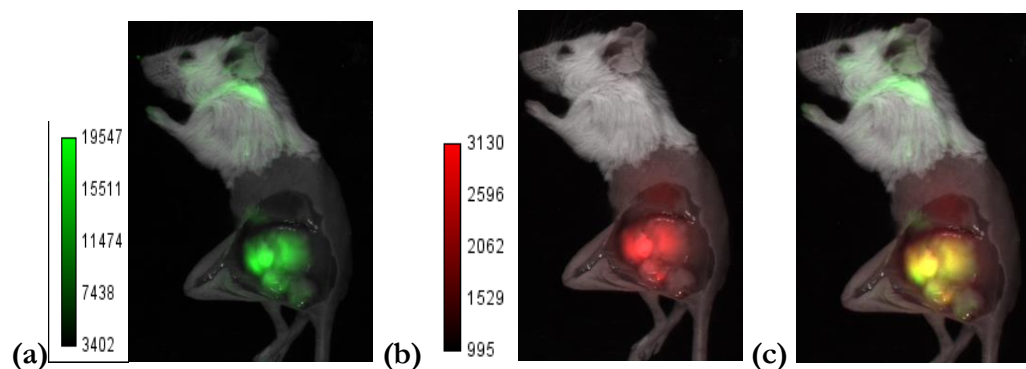

Figure 3.12 LS301 and PpIX fluoresence overlap in subcutaneous DBT mouse after skin deflected. (a) PpIX fluoresence (green) by 630nm/700nm filtered light (b) LS301 fluoresence (red) by 760nm/700nm filtered light. (c) Merged LS301 and PpIX fluorescence by Image J.
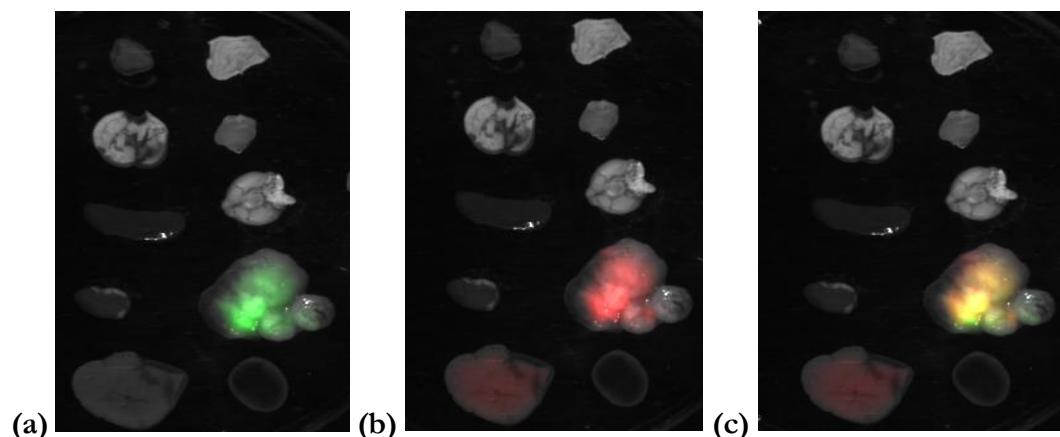
Figure 3.13 Biodistribution of PpIX and LS301 fluorescence in subcutaneous DBT mouse. (a) PpIX fluoresence (green) by 630nm/700nm filtered light (b) LS301 fluoresence (red) by 760nm/700nm filtered light. (c) Merged LS301 and PpIX fluorescence by Image J. On the left column, from the top to bottom: heart, lung, spleen, kidney and liver, respectively. On the right column, from the top to bottom: skin, muscle, brain, tumor and blood, respectively.

Figure 3.14 5-ALA induced PpIX fluoresence biodistribution by three different excitation/emission filters, 420nm/ 600nm (purple), 510/600nm (green) and 630nm/700nm (orange), repectively.

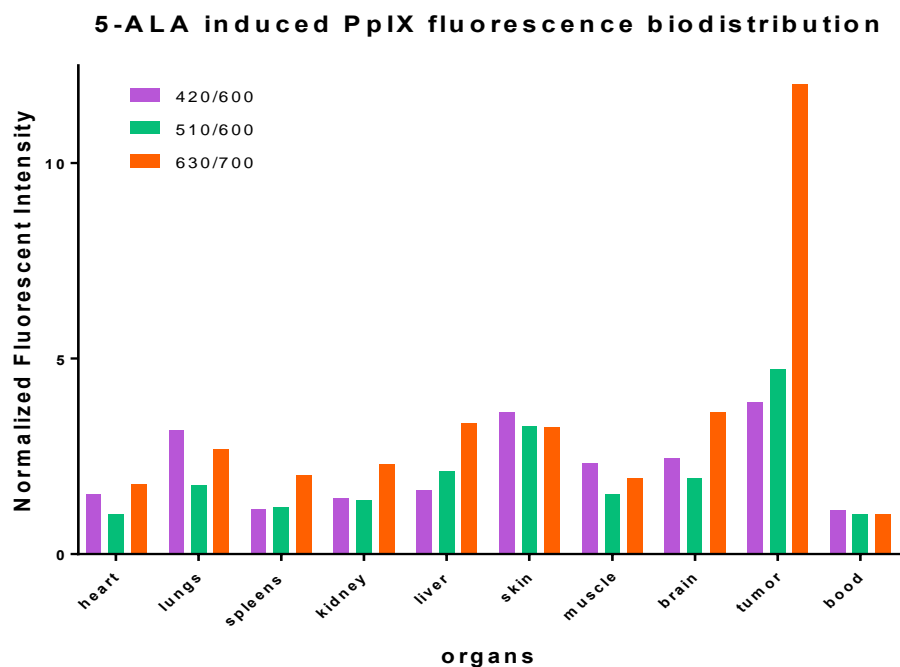LS301 and PpIX also shows co-localization at some sites in the DBT tumor tissue slice of subcutaneous DBT mouse. The reason that LS301 fluoresence is very weak is that most of LS301 had been cleared by mouse after six days post injection of LS301. H&E staining confirmed the tissue cells which have fluorescence are tumor cells.
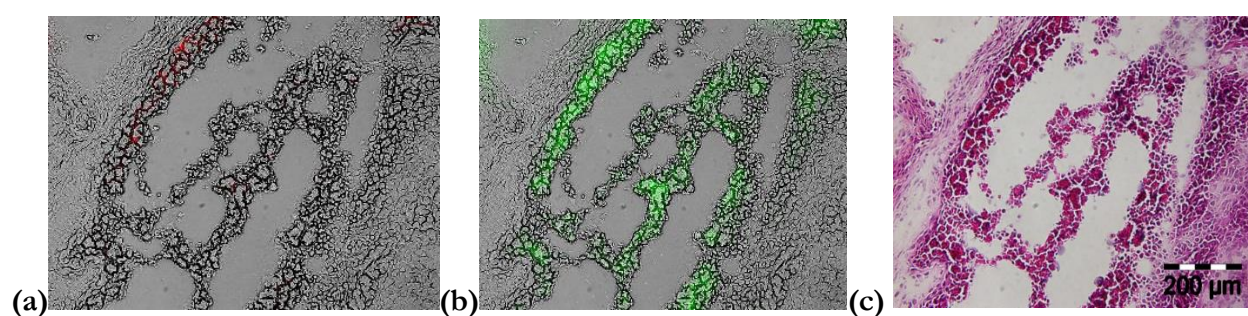

(a) **(b)** **(c)**

Figure 3.15 LS301 and PpIX fluoresence in tumor tissue slice of subcutaneous DBT mouse. (a) LS301 fluorescence (red) under CY5 channel on Epi-fluoresence microscope. (b) PpIX fluorescence (green) under FITC channel on Epi-fluoresence microscope. (c) H&E staining of the tissue slice of interest.

Ex/Em (nm/nm)	420/600	510/600	630/700	760/830
Tumor-to-muscle ratio	1.36	2.36	10.8	23.8

Table 3.1 Tumor-to-muscle ratio of fluorescnece at different filters.

We also tried to use Pearl imager system to check PpIX fluorescnece. In fig. 3,16, PpIX fluorescece is not distinct by channel 700 on Pearl imager after 7hours injection of 5-ALA. This can be explained that PpIX has very weak absoption at 685 nm excitation wavelength. Sencond injection of 5-ALA was performed. The PpIX flurescence was recorded in 24hours. At 24 hours post injection of 5-ALA, weak PpIX signal on channel 700 is shown in fig. 3.18. PpIX fluorescence is more distinct after the skin was deflected at the tumor area. The pearl imager system also confirmed the colocalization of LS301 and PpIX in subcutaneous DBT mouse (fig. 3.20)

Figure 3.16 PpIX fluorescence is not obvious at 4h (a), 5.5h (b), 6h (c) and 7h (d) post injetion of 5-ALA on subcutaneous DBT mouse by channel 700 on Pearl imager. The excitation wavalength is 685nm and emission wavelength is 720nm on channel 700.

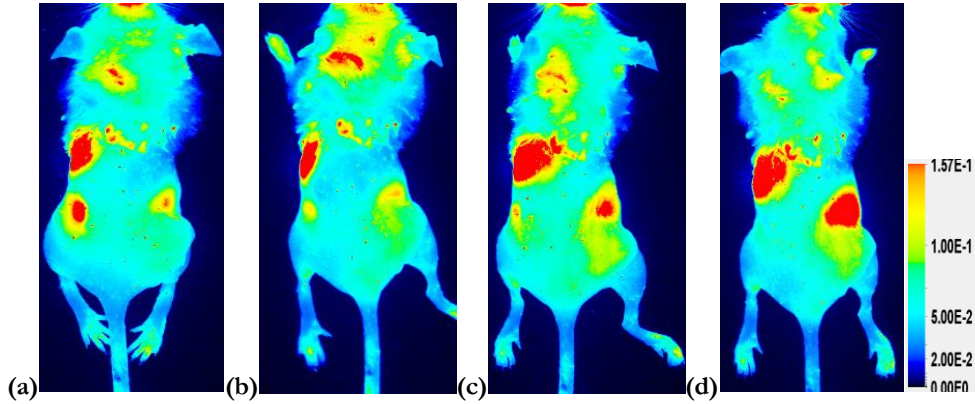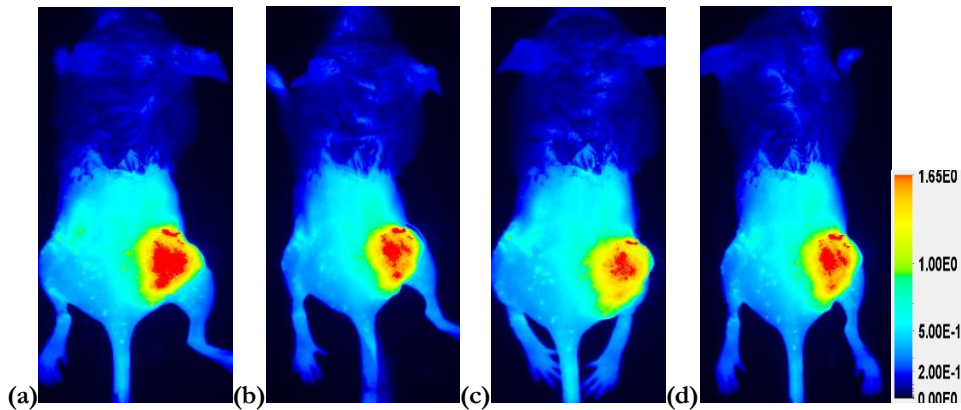**Figure 3.17 LS301 fluorescence is obvious at 4h (a), 5.5h (b), 6h (c) and 7h (d) post injetion of 5-ALA in subcutaneous DBT mouse by channel 800 on Pearl imager. The excitation wavalength is 785nm and emission wavelength is 820nm on channel 800.**
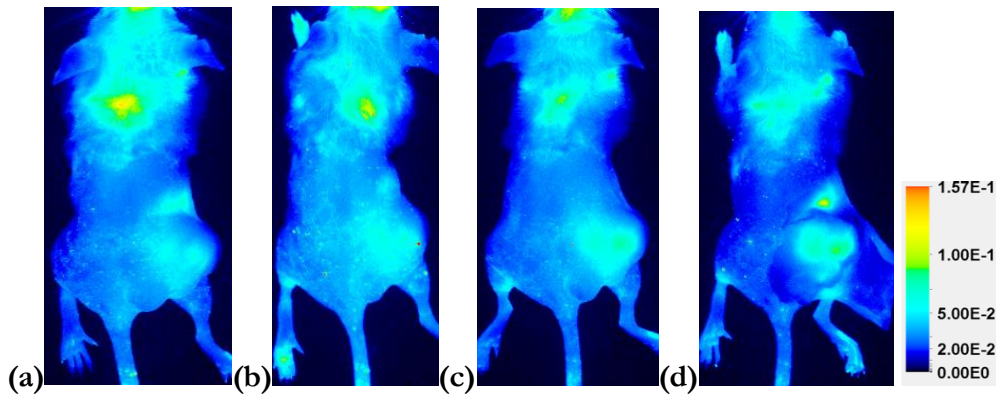
Figure 3.18 PpIX fluorescence is obvisous at 24h post injection of 5-ALA and at tumor area with skin deflected. Fluorescnee under channel 700 at 2hours PI (a), 9 hous PI (b), 24 hours PI (c) of 5-ALA in subcutaneous DBT mouse and deflected skin (d) by channel 700 on Pearl imager. The excitation wavalength is 685nm and emission wavelength is 720nm on channel 700.

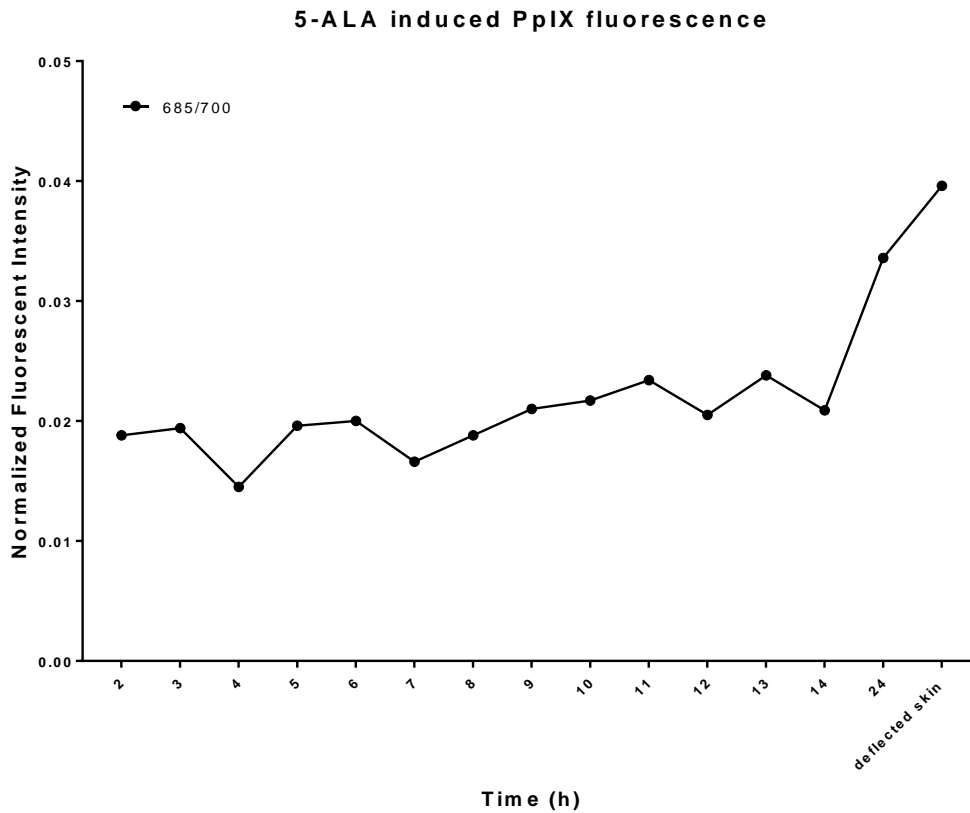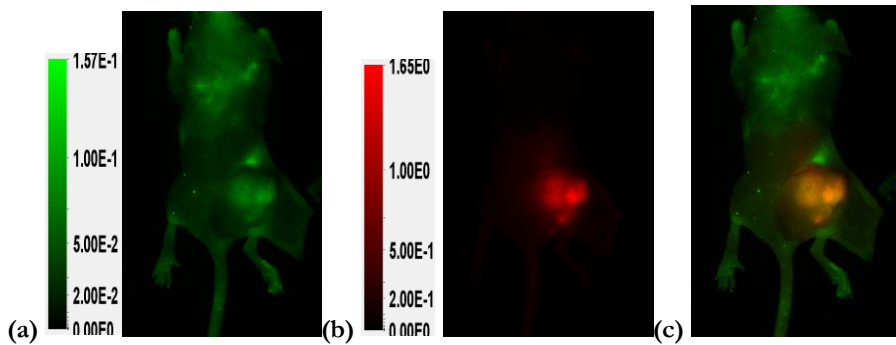**Figure 3.19 5-ALA induced PpIX fluoresence intensity at different time by channel 700 on Pearl imager. PpIX fluoresence when the skin was deflected was recorded as well.**
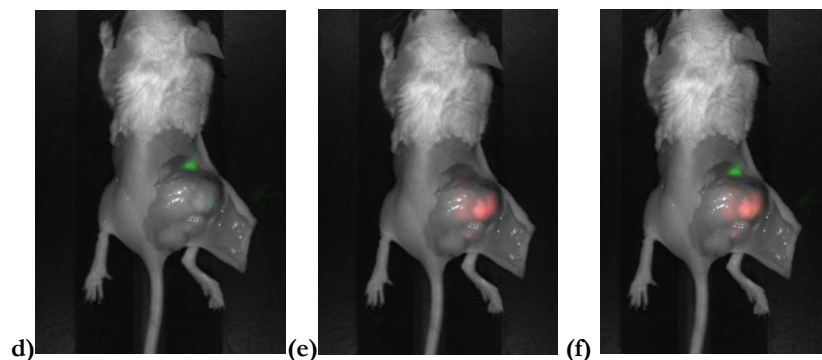
Figure 3.20 co-localization of LS301 (red channel 800)and PpIX (green channel 700) were analyzed by Pearl imager.

Overall, the best excitation and emission filter for observing PpIX fluoresence in subcutanous mouse mode is 630nm/700nm. And the PpIX fluoresence started to be distinct after 9 hours from 100uL 50mg/mL 5-ALA injection. Without the block of skin, PpIX fluoresence intensity reached maximum. Furthermore, overlap of LS301 and PpIX fluoresence indicated the colocalizatio of LS301 and PpIX in subcutanous DBT mouse model.

3.3.2   Subcutaneous and Orthotopic U87 mice

630/700nm excitation and emission filter has been confirmed as the best choice for detecting PpIX fluorescence in subcutaneous mice model. The previous study in vitro also showed that U87 does not has a good uptake of 5-ALA and LS301 as DBT cells. Thus it is reasonable that PpIX fluorescence was not detectable on Brucker imaging system when the tumor tissue was not exposed under the 630nm excitation light. PpIX fluorescence became distinct in subcutaneous U87 mouse after its skin was deflected under 630nm/700nm. However, 630/700nm filter did not work well for orthotopic U87 mice after the skull open. In contrast, PpIX fluorescence signal in orthotopic U87 mouse was visualized by 510nm/600nm filter (fig 3.24). PpIX fluorescence ratio of tumor to muscle is less than 1 which means that PpIX is a low contrast for subcutaneous U87 mouse (table 3.2). The LS301 fluorescence ratio of tumor to muscle in subcutaneous U87 mouse was over 3.5. Apparently,

LS301 serves as a higher contrast comparing to PpIX. Thereby, LS301 has the potential to be play an important role in guiding PpIX imaging surgery for glioblastoma tumor patients.
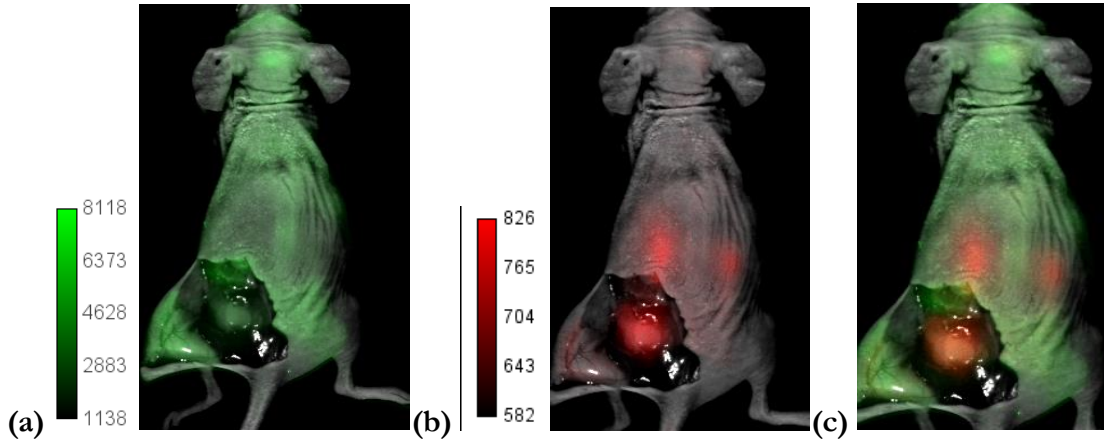

Figure 3.20 LS301 and PpIX fluoresence overlap in subcutaneous U87 mouse after skin deflected. (a) PpIX fluoresence (green) by 630nm/700nm filtered light (b) LS301 fluoresence (red) by 760nm/700nm filtered light. (c) Merged LS301 and PpIX fluorescence by Image J.

Figure 3.21 Biodistribution of PpIX and LS301 fluorescence in subcutaneous U87 mouse. (a) PpIX fluoresence (green) by 630nm/700nm filtered light (b) LS301 fluoresence (red) by 760nm/700nm filtered light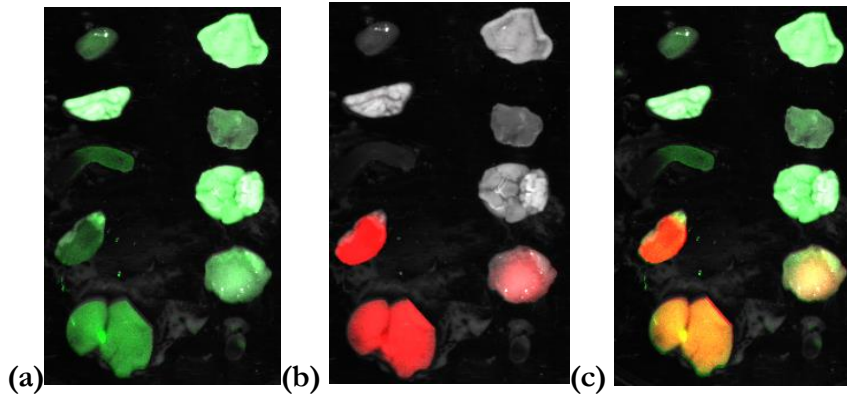. (c) Merged LS301 and PpIX fluorescence by Image J. On the left column, from the top to bottom: heart, lung, spleen, kidney and liver, respectively. On the right column, from the top to bottom: skin, muscle, brain, tumor and blood, respectively.

LS301 vs PpIX fluprescence U87-MG in vivo
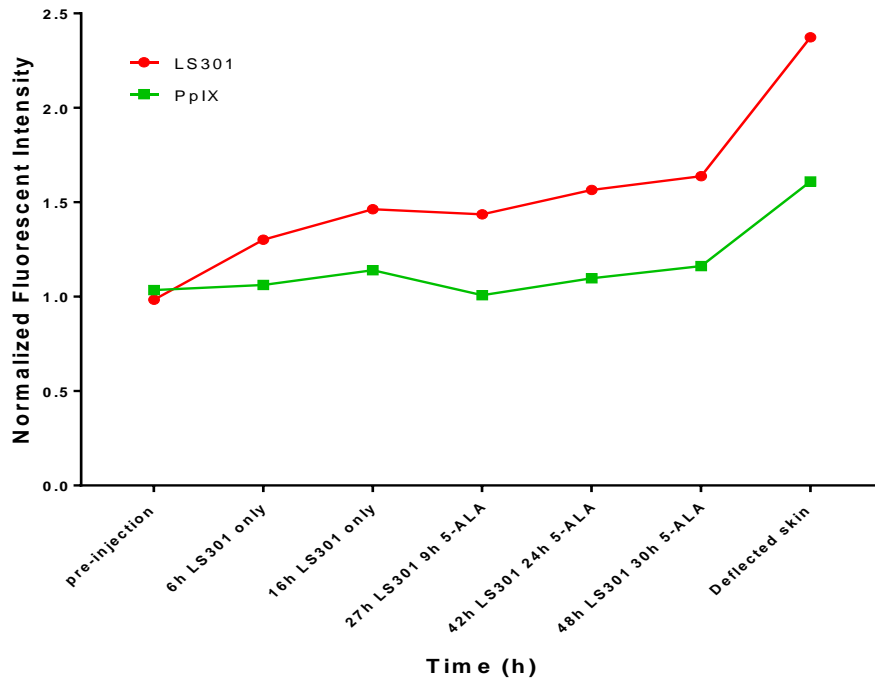

Figure 3.22 LS301 and PpIX fluorescne intensity at different post injection hours. LS301 fluorescnece is indicated by solid red line and PpIX fluorescence is indicated by solid green line, respectively.
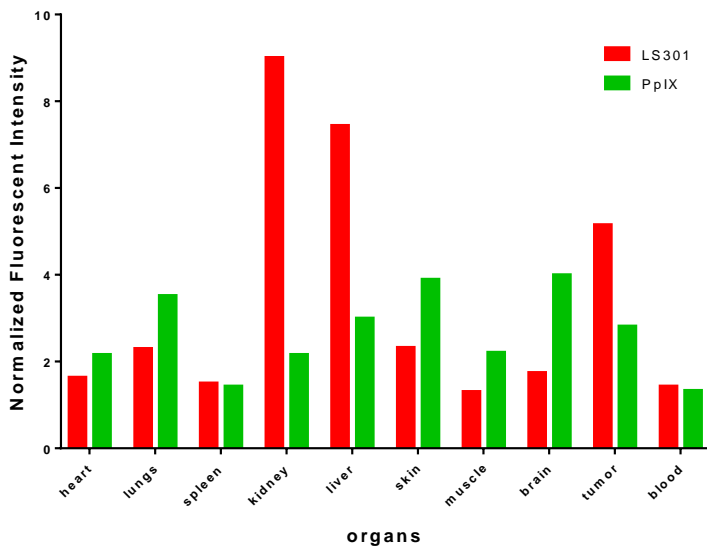
LS301 vs PpIX fluorescence biodistribution

Figure 3.23: 5-ALA induced PpIX fluoresence biodistribution by three different excitation/emission filters, PpIX fluorescence is shown in green bar and LS301 fluorescence is shown in red bar , repectively.

Ex/Em (nm/nm)	630/700	760/830
Tumor-to-muscle ratio	0.78	3.09

Table 3.2 Tumor-to-muscle ratio of fluorescnece at different filters. PpIX fluorescence ratio of tumor to musle is recoded by 630nm/700nm filter, and LS301 ratio is recorded by 760nm/830nm filter, respectively.
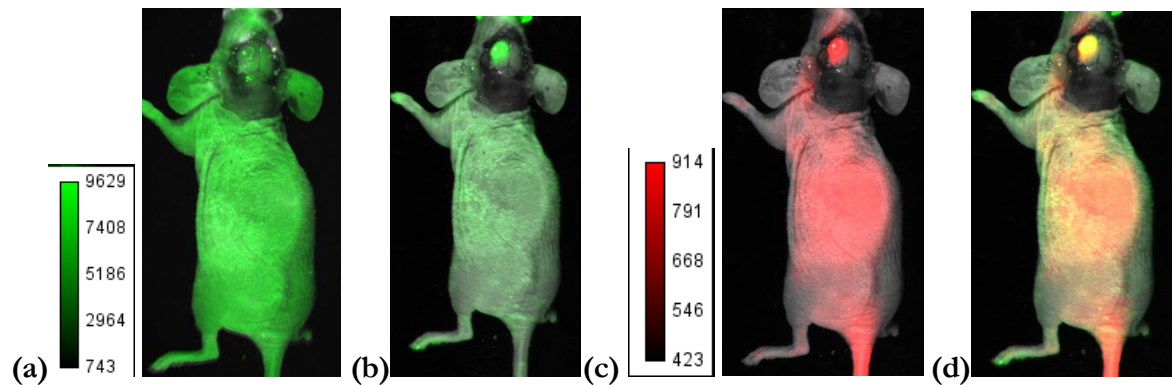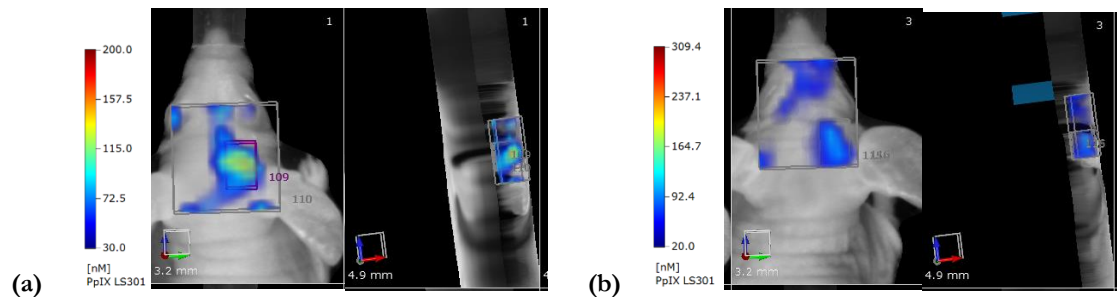

Figure 3.24 PpIX and LS301 fluoresence in orthotopic U87 mouse model. (a) PpIX fluoresence is weak by 630/700nm filter on brucker imaging system. (b) PpIX fluorescence by 510/600 nm filter. (c) LS301 fluorescence by 760/830nm filter. (d) Merged LS301 and PpIX in orthotopic U87 mouse by Image J analysis.
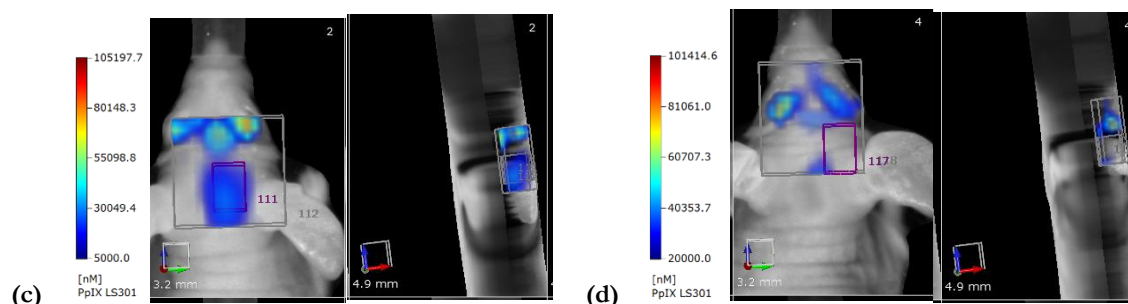
Figure 3.25 LS301 and PpIX fluoresence on FMT system. (a) and (c) represnet front view and side view of LS301 and PpIX fluorescence observed at 22 hours PI of LS301 and 6hours PI of 5-ALA by 790 channel and 635 channel, respectively. (b) and (d) front view and side view of LS301 and PpIX fluorescence observed at 46 hours PI of LS301 and 24 hours PI of 5-ALA by 790 channel and 635 channel, respectively.

Pearl imager and Brucker imaging system only can provide 2D image. FMT, a small-animal fluorescence in vivo imaging system, was introduced to provide 3D reconstructed image. Channel 790 (excitation 790nm/emission 805nm) was used to detect LS301 fluorescence. PpIX have a sbsorption peak at 635nm wavelength but a low fluorescence at 660nm emission filter. Thus, channel 635 (excitation 635nm/emission 660nm) still is not the best choice for PpIX fluorescence. LS301 and PpIX fluorescence co-localize in orthotopic U87 mousea at 22 hours LS301 and 6 hours 5-ALA. But PpIX fluorescence is not shown at 24 hours PI of 5-ALA. In summary, LS301 and PpIX fluorescence still show co-localization in subcutaneous and orthotopic U87 mouse model. 510nm/600nm filter on brucker gave higher PpIX fluorescence in orthotopic U87 mouse model rather than 630/700nm, the optimal protocol for subcutaneous mouse model.

3.4   LS301 guided PpIX PDT in mice model

3.4.1   PDT setup

660nm wavelength laser was used to irradiate the tumor spot in the subcutaneous U87 mice model after 6h post injection of 100uL, 50mg/mL 5-ALA. The distance between LED len and mice tumor

was set to 10cm to achieve an irradiation intensity of 72mW/cm². The exposure time was 20 minutes [12]. The custom PDT setup in our lab is shown in fig. 3.26.
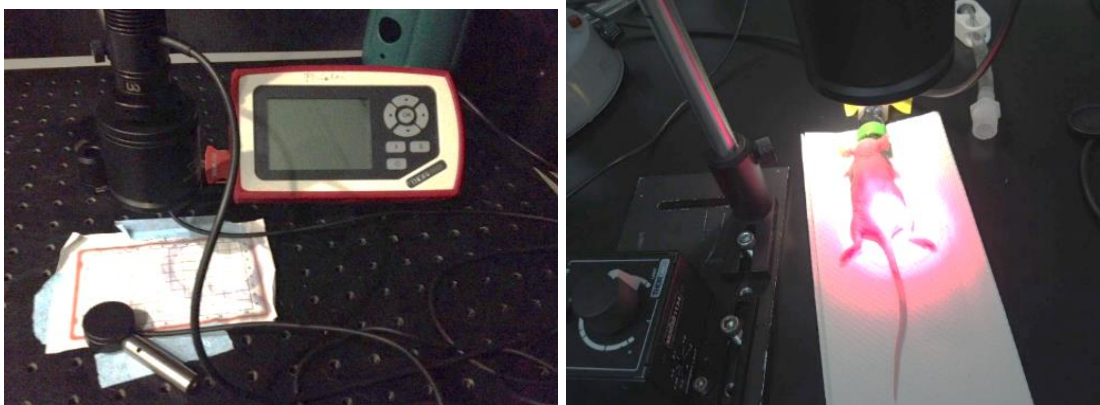

Figure 3.26 PDT setup

3.4.2   Tumor growth rate after PDT

The tumor size calculation formula used to calculate subcutaneous tumor tissue sie is shown in equation 1 [13].

$$V= \frac{(\textbf{long length})\times(\textbf{short length}^2)}{2}$$ **Equation 1**
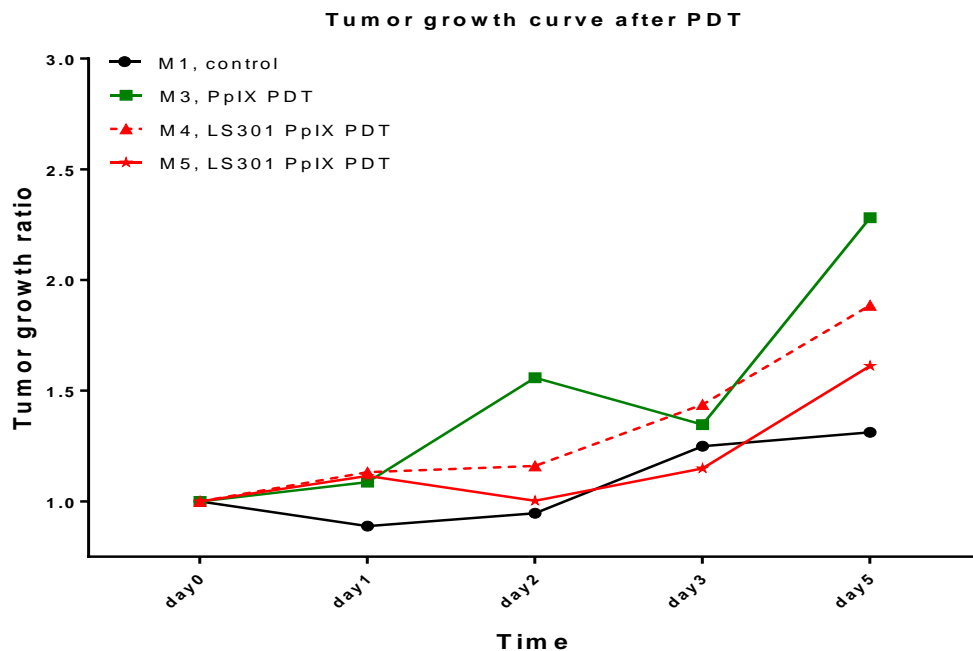
Figure 3.27 tumor growth ratio after PDT on subcutaneous U87 mice model.

Subcutaneous U87 tumors implanation in mouse M2 was failed. The tumor growth ratios of other 4 subcutaneous U87 mice are shown in fig. 3.27. Tumor was continuouly growing in both subcutaneous U87 mice treated with PpIX PDTor LS301-PpIX PDT. This negative result might be caused by the limitation of PDT setup. In most research studies, 635nm laser provides the most efficient PpIX PDT and the ideal irradiation intensity is 100 mW/cm^2. However, 660nm laser was used in our PDT trials and the PDT radiation power was not strong enough. But LS301 PpIX PDT showed restriction of tumor growth comparing to PpIX PDT in the absence of LS301. We might assume that LS301 may improve PpIX mediated PDT.

3.5   Future plans

In the next step, we will work in tracking LS301 and PpIX target sits in various organelles of brain cell lines. And we will perform PDT using 635nm laser to brain cell lines and mice models. Also, the

amount of mice is not sufficient in this thesis research study; thus, we will also repeat in-vivo study with more mice.

References

[1] Siegel, R. L., Miller, K. D. and Jemal, A. (2017), Cancer statistics, 2017. CA: A Cancer Journal forClinicians, 67: 7–30. doi:10.3322/caac.21387

[2] John, A. H., Stergios, Z., and Mark, W. K. (2012), Asia-pacific journal of clinical oncology, 2012. Pediatric neuro-oncology: Current Status and Future Directions, 8: 223-231. doi:10.1111/j.1743-7563.2012.01558.x

[3] Seppa, N. (2015). Body & brain: New cancer drugs can wake up sleeping killer T cells: Frontline immune system fighters, often evaded by tumors, might now resume the attack. Science News, 188(1), 14-15. doi:10.1002/scin.2015.188001017.

[4] "The Operation"The Operation to Remove a Brain Tumor in Israel, the Cost and Reviews Assuta." , The Cost and Reviews, Assuta, assuta.clinic/otdeleniya/neyrohirurgiya/operaciya-po-udaleniyu-opuholi-golovnogo-mozga.html.

[5] Mondal, S. B. et al. Binocular Goggle Augmented Imaging and Navigation System provides real-time fluorescence image guidance for tumor resection and sentinel lymph node mapping. Sci. Rep. 5, 12117; doi: 10.1038/srep12117 (2015).

[6] Koizumi N, Harada Y, Minamikawa T, Tanaka H, Otsuji E, Takamatsu T. Recent advances in photodynamic diagnosis of gastric cancer using 5-aminolevulinic acid. World J Gastroenterol 2016; 22(3): 1289-1296.

[7] Teng L., et al. (2013)Current application of 5-ALA in glioma diagnostics and therapy. Oncology 2013, doi: 10.5772/52428.

[8] Pollack, I.F., Pediatric brain tumors. Seminars in Surgical Oncology, 1999. 16(2): p. 73-90.

[9] Mondal, S.B., et al., Binocular Goggle Augmented Imaging and Navigation System provides real-time fluorescence image guidance for tumor resection and sentinel lymph node mapping. Sci Rep, 2015. 5: p. 12117.

[10]Nadia Naghavi, Mohammad Hossein Miranbaygi, Ameneh Sazgarnia, "Determination of Protoporphyrin IX Concentration in Photodynamic Therapy Based on Fluorescence Measurement", Computer and Electrical Engineering 2009. ICCEE '09. Second International Conference on, vol. 2, pp. 315-317, 2009.

[11]J. A. Rissell et al. " Characterization of Fluoresence Lifetime of photofrin and Delta-

Aminolevulinic Acid Induced Photoporphyrin IX in Living Cells Using Signle-and Two-photon Excitation," in IEEE Journal of Selected Topics in Quantum Electronics, vol 14, no.1, pp. 158-166, Jan,-feb. 2008. doi: 10.1109/JSTQE.2007.912896.

[12] Xie, Y., Wei, Z., Zhang, Z., Wen, W., & Huang, G. (2009). Effect of 5-ALA-PDT on VEGF and PCNA expression in human NPC-bearing nude mice. Oncology Reports, 22, 1365-1371. https://doi.org/10.3892/or_00000576

[13] Jensen, M.M., Jorgensen, J. T., Binferup, T., and Kjar A (2008) Tumor volume in subcutaneous mouse xenografts measured by micro CT is more accurate and reproducible than determined by ^{18}F-FDG-microPET or external caliper. BMC medical imaging, 8, 16. http://doi.org/10.1186/1471-2342-8-16